Mass lumping models of the linear diffusion equation

T. V. HROMADKA II

Department of Civil Engineering, University of California, Irvine, California 92717, USA

G. L. GUYMON

Department of Civil Engineering, University of California, Irvine, California 92717, USA

The nodal domain integration method is used to develop a numerical model of the linear diffusion equation. The nodal domain integration approach is shown to represent an infinity of finite element mass matrix lumping schemes including the Galerkin and subdomain integration versions of the weighted residual method and an integrated finite difference method. Neumann, Dirichlet and mixed boundary conditions are accommodated analogous to the Galerkin finite element method. In order to reduce the overall integrated approximation relative error, a mass matrix lumping formulation is developed which is based on the Crank-Nicolson time advancement approximation. The optimum mass lumping factors are found to be strongly related to the model timestep size.

INTRODUCTION

Engineers and scientists are increasing their reliance on numerical methods to approximately solve differential equations of boundary and/or initial value problems such as occur in the study of transport processes. Usually, the numerical approaches to finite difference or finite elements are employed. These techniques discretize an assumed continuum-domain of definition into finite elements or control volumes, and the governing partial differential equation (PDE) is approximated in the continuum by trial functions which fully or partially satisfy the PDE boundary conditions. Choosing suitable points called 'nodes' within the several finite elements or control volumes, the variable in the PDE is written as a linear combination of specified interpolation functions and the values of the variable or its various derivatives at the nodal points. Using variational or weighted residual methods, the governing flow process PDE is approximated by a system of linear equations as functions of nodal point values.

There are numerous numerical approaches available; however, usually either the Galerkin finite element or finite difference methods are used to solve PDE's such as diffusion problems.[1] Alternative numerical approaches have been investigated by several workers. Narasimhan[2-4] examined fluid flow in porous media and the diffusion problem by a control volume approach which is based on a finite difference method. Patankar[5] also presented a triangular finite difference control volume model for a heat transfer diffusion problem. Both modeling efforts can be expressed in a finite element matrix form such as described in Hromadka *et al.*[6]

The control volume models are analogous to finite element mass matrix lumping models such as described by Kikuchi.[7] That is, the control volume approach essentially results in the formulation of a finite element mass matrix which is lumped or diagonal. Fried and Malkus[8] use numerical integration to form mass matrix lumping schemes with the optimal rate of energy convergence retained. Other formulations include a consistent diagonal mass matrix finite element model[9] which also produces a diagonal mass matrix similar to the lumped class. This type of formulation is extended to two-dimensional finite elements using orthogonal base functions.[10] Another examination of mass lumped and consistent mass matrices is given by Surana[11] for the special problem of a three dimensional structural beam element.

The above mass lumping models and control volume approaches can be shown to be essentially analogous to the basic integrated finite difference method developed by Spalding[12] for transport problems. The integrated finite difference method is oftentimes acclaimed for its ease of model developed and simple solution of the integrated version of the governing PDE.[13] Additionally for many problems, the finite difference method (often referred to as the control volume approach) may produce 'better' results than the Galerkin finite element method[14] although the opposite can be true depending on the class of problem being solved.[15] The subdomain integration method is also referred to as the control volume approach and can be shown to result in another mass matrix which is consistent,[16] but yet is not diagonal. Thus the modeler is left to choose between several different numerical modeling methods which are in reality essentially similar to each other when written in a simple finite element matrix form.

The main objectives of this paper are twofold. First, the paper will briefly review the development of a one-dimensional nodal domain integration (NOI) numerical model of the diffusion problem. This model development is derived in detail in previous papers,[6,17] and only the major steps of the derivation are included in this paper for the reader's convenience. Extension of the one-dimensional model to a

Received September 1982. Written discussion closes August 1983.

0309-1708/83/020079-09$2.00

two- and three-dimensional formulation follows from the one-dimensional model derivation. Each of the resulting numerical models are shown to represent the often-used Galerkin and subdomain integration models and an integrated finite difference model as well as an infinity of other nodal weighting schemes. The global matrix systems are shown to satisfy both Dirichlet, Neumann and mixed boundary conditions similar to the Galerkin approach.

The second objective of this paper is to determine a nodal weighting relation which has a high probability of reducing integrated relative error. The proposed nodal weighting (mass lumping) method was determined by curve-fitting numerous optimized mass-lumping factors developed by trial and error in the comparison of approximation results to analytical results for several classical linear PDE boundary value problems where analytical solutions exist. Based on the comparison of modeled results and corresponding errors, general patterns were identified which may lead to the best numerical solution to the general problem.

The proposed mass lumped scheme is based on the subdomain integration (control volume) approach as applied to an actual solution trial function of the governing PDE. The trial function assumed is the principal eigenfunction of the Fourier series expansion solution to a special case of the diffusion problem which approximates the control volume in the global model. Since all but one of the eigenfunctions essentially disappear in the solution of the PDE after a short time, the resulting model solution generally produces better approximations for the diffusion problem than any of the more popular domain numerical methods. The diffusion problems considered are only for the linear class of PDE. Extension of nonlinear problems is not straightforward due to the evaluation of a nonlinear diffusivity at the boundary of the control volume. Further research is required to extend these methods to nonlinear problems.

All of the above models can be written in terms of a single nodal domain integration numerical statement for each nodal point value. The numerical statement is written as a function of a single mass matrix lumping factor η, and results in a representation of domain models in finite element matrix form.

DOMAIN APPROXIMATIONS OF PARABOLIC EQUATIONS

In this section, a brief summary of domain numerical model derivations is presented for the well known Galerkin finite element and the integrated finite difference models. Also presented is the subdomain integration model derivation. Although the derivations are well known, some particular steps are presented here in order to determine some of the many similarities between the various models. Each numerical model is then written in a finite element matrix form which indicates the degree of mass lumping each model involves. All of the models are then combined into one unifying finite element matrix formulation (or nodal domain integration model) as a function of the degree of mass matrix diagonalization. The resulting NDI statements represent an infinity of possible mass matrix lumping models of which the more popular domain methods are but special cases. In the following section, an improved nodal weighting scheme is developed which, for the problems tested, reduce integrated relative error for one-dimensional linear diffusion problems.

Galerkin method of weighted residuals

The general parabolic equation describing a linear one-dimensional diffusion process is

$$\alpha \frac{\partial \phi}{\partial t} - \frac{\partial^2 \phi}{\partial x^2} = 0, \quad x \in \Omega \tag{1}$$

where ϕ is the volumetric concentration; (x, t) are spatial and temporal coordinates; α is a diffusivity parameter; and Ω is the problem global domain with global boundary Γ.

The finite element approach[18] discretizes the global domain into the union of finite elements by

$$\Omega \equiv \cup \Omega^e \tag{2}$$

The domain is expressed as the union of domain and boundary

$$\Omega \equiv \Omega \cup \Gamma \tag{3}$$

$$\Omega^e \equiv \Omega^e \cup \Gamma^e \tag{4}$$

where

$$\Omega^e \cap \Omega^{e+1} = \Gamma^e \cap \Gamma^{e+1} \tag{5}$$

The PDE variable ϕ is assumed approximated in each Ω^e by a linear trial function ϕ^e defined by

$$\phi^e \equiv \Sigma N_j(x)\, \phi_j^e \tag{6}$$

where $N_j(x)$ is an assumed linear polynomial shape function of nodal point j and ϕ_j^e is a nodal point value associated to element Ω^e. The Galerkin weighted residual process approximates (1) in each Ω^e by setting

$$\int_{\Omega^e} \left(\frac{\partial^2 \phi}{\partial x^2} - \alpha \frac{\partial \phi}{\partial t} \right) N_j \, d\Omega \equiv 0, \quad e = 1, 2, \ldots \tag{7}$$

where boundary conditions of Neumann or Dirichlet are assumed on global boundary Γ. Integrating (7) by parts gives

$$\int_{\Omega^e} \left(\frac{\partial^2 \phi}{\partial x^2} - \alpha \frac{\partial \phi}{\partial t} \right) N_j \, d\Omega = \left(\frac{\partial \phi}{\partial x} N_j \right) \Big|_{\Gamma^e} - \int_{\Omega^e} \left(\frac{\partial \phi}{\partial x} \frac{dN_j}{dx} + \alpha \frac{\partial \phi}{\partial t} N_j \right) d\Omega \tag{8}$$

To conserve mass-flux continuity between Ω^e, it is assumed that

$$\sum_e \left(\frac{\partial \phi}{\partial x} N_j \right) \Big|_{\Gamma^e} \equiv \left(\frac{\partial \phi}{\partial x} \right) \Big|_{\Gamma} \tag{9}$$

For a Neumann (natural) boundary condition on global boundary Γ,

$$\left(\frac{\partial \phi}{\partial x} \right) \Big|_{\Gamma} \equiv 0 \tag{10}$$

For Neumann or Dirichlet boundary conditions specified on global domain Γ, the Galerkin analog for local element Ω^e reduces to

$$\int_{\Omega^e} \left(\frac{\partial^2 \phi}{\partial x^2} - \alpha \frac{\partial \phi}{\partial t} \right) N_j \, d\Omega = - \int_{\Omega^e} \left(\frac{\partial \phi}{\partial x} \frac{dN_j}{dx} + \alpha \frac{\partial \phi}{\partial t} N_j \right) d\Omega \tag{11}$$

For the linear trial function ϕ^e in Ω^e,

$$\phi \cong \phi^e = \left(\frac{l^e - y}{l^e}\right)\phi_e + \left(\frac{y}{l^e}\right)\phi_{e+1} \tag{12}$$

where y is a local coordinate in Ω^e, $dy = dx$; $l^e = (x_{e+1} - x_e)$; $(\phi_e, \phi_{e+1}) \equiv \phi^e$; and x_e is the spatial coordinate of node e. Substituting (12) into (11) gives a Galerkin analog for local element Ω^e

$$0 \equiv \int_{\Omega^e} \left(\frac{\partial \phi^e}{\partial x}\frac{dN_j}{dx} + \alpha^e \frac{\partial \phi^e}{\partial t} N_j\right) d\Omega, \quad j = e, \quad e+1 \tag{13}$$

For ϕ^e linear, all gradients are constant giving

$$0 \equiv \frac{\partial \phi^e}{\partial x}\int_{\Omega^e} \frac{dN_j}{dx}\, d\Omega + \alpha^e \frac{\partial}{\partial t}\int_{\Omega^e} \phi^e N_j\, d\Omega, \quad j = e, \quad e+1 \tag{14}$$

In matrix notation, the linear system of equations approximating the governing PDE in local element Ω^e is

$$\mathbf{S}^e \phi^e + \mathbf{P}^e[2]\dot{\phi}^e = \frac{\partial \phi^e}{\partial x}\int_{\Omega^e} \frac{dN_j}{dx}\, d\Omega + \alpha^e \frac{\partial}{\partial t}\int_{\Omega^e} \phi^e N_j\, d\Omega$$

where;

$$\mathbf{S}^e = \frac{1}{l^e}\begin{bmatrix} 1 & -1 \\ -1 & 1 \end{bmatrix} \tag{16}$$

$$\mathbf{P}^e[2] = \frac{\alpha^e l^e}{6}\begin{bmatrix} 2 & 1 \\ 1 & 2 \end{bmatrix} \tag{17}$$

and

$$\dot{\phi}^e = \frac{\partial}{\partial t}(\phi^e)$$

Subdomain integration

The subdomain integration method discretizes the global domain Ω into subdomains (control volumes) where

$$\Omega = \cup R_j \tag{18}$$

Generally, the subdomains are defined such that R_j is somewhat centered about nodal point j and

$$x_j \in R_j \tag{19}$$

$$x_k \notin R_j, \quad k \neq j \tag{20}$$

$$R_j \cap R_k = \Gamma_j \cap \Gamma_k \tag{21}$$

$$R_j \equiv R_j \cup \Gamma_j \tag{22}$$

For the one-dimensional parabolic PDE problem, Ω is discretized into subdomains which overlap continuous finite elements from mid-element to mid-element.

The subdomain integration weighted residual approach averages the approximation error in estimating the governing PDE in R_j by the formulation

$$\int_{\Omega} \left(\frac{\partial^2 \phi}{\partial x^2} - \alpha \frac{\partial \phi}{\partial t}\right)\omega_j\, d\Omega \equiv 0 \tag{23}$$

where boundary conditions of Neumann or Dirichlet are specified on global boundary Γ. From the discretization of Ω,

$$\int_{\Omega} \left(\frac{\partial^2 \phi}{\partial x^2} - \alpha \frac{\partial \phi}{\partial t}\right)\omega_j\, d\Omega = \int_{R_j} \left(\frac{\partial^2 \phi}{\partial x^2} - \alpha \frac{\partial \phi}{\partial t}\right)\omega_j\, d\Omega \tag{24}$$

where

$$\omega_j \equiv \begin{cases} 1, & x \in R_j \\ 0, & \text{otherwise} \end{cases} \tag{25}$$

Thus,

$$\int_{\Omega} \left(\frac{\partial^2 \phi}{\partial x^2} - \alpha \frac{\partial \phi}{\partial t}\right)\omega_j\, d\Omega = \int_{R_j} \left(\frac{\partial^2 \phi}{\partial x^2} - \alpha \frac{\partial \phi}{\partial t}\right) d\Omega \tag{26}$$

The subdomain and finite element discretization of Ω can be rewritten in terms of a nodal domain Ω_j^e discretization of Ω by

$$\Omega_j^e \equiv \Omega^e \cap R_j \tag{27}$$

A one-dimensional discretization of global domain Ω by each of the three approaches are shown in Fig. 1. From the definition of the nodal domain, a subdomain R_j would be the union of each Ω_j^e, that is

$$R_j = \cup \Omega_j^e \tag{28}$$

and the finite element Ω^e is given by

$$\Omega^e = \cup \Omega_j^e, \quad j \in S^e \tag{29}$$

where S^e is the set of nodal point numbers associated to finite element Ω^e

$$S^e \equiv \{j : \Omega^e \cap \Omega_j^e \neq \{\emptyset\}\} \tag{30}$$

Consequently, a finite element matrix system can be determined for a subdomain integration model by noting that

$$\int_{R_j} \left(\frac{\partial^2 \phi}{\partial x^2} - \alpha \frac{\partial \phi}{\partial t}\right) d\Omega = \int_{\Omega_j^e} \left(\frac{\partial^2 \phi}{\partial x^2} - \alpha \frac{\partial \phi}{\partial t}\right) d\Omega \tag{31}$$

In terms of finite element Ω^e,

$$\int_{\Omega^e} \left(\frac{\partial^2 \phi}{\partial x^2} - \alpha \frac{\partial \phi}{\partial t}\right)\omega_j\, d\Omega = \int_{\Omega_j^e} \left(\frac{\partial^2 \phi}{\partial x^2} - \alpha \frac{\partial \phi}{\partial t}\right) d\Omega, \quad J \in S^e \tag{32}$$

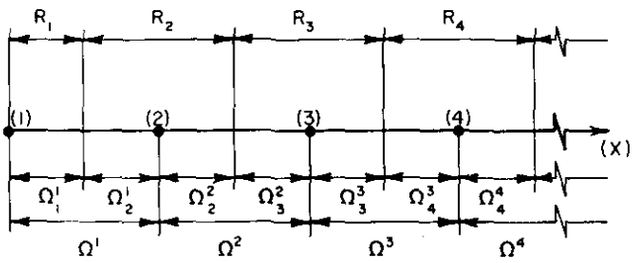

Figure 1. One dimensional discretization of global domain Ω showing nodal points (1), finite elements Ω^e, subdomains R_j, nodal domains Ω_j^e and nodes ●

Integrating equation (32) by parts gives:

$$\int_{\Omega_j^e}\left(\frac{\partial^2\phi}{\partial x^2}-\alpha\frac{\partial\phi}{\partial t}\right)d\Omega=\left(\frac{\partial\phi}{\partial x}\right)\Big|_{\Gamma_j^e\cap\Gamma^e}+\left(\frac{\partial\phi}{\partial x}\right)\Big|_{\Gamma^e-\Gamma_j^e\cap\Gamma^e}-\int_{\Omega_j^e}\alpha\frac{\partial\phi}{\partial t}d\Omega,\quad j\in S^e \tag{33}$$

where $S^e=(e,\ e+1)$; and Γ_j^e is the boundary of nodal domain Ω_j^e. Similar to the Galerkin approach, flux continuity is assumed between finite elements and Neumann or Dirichlet boundary conditions are assumed on global boundary Γ giving

$$\sum_e\left(\frac{\partial\phi}{\partial x}\right)\Big|_{\Gamma_j^e\cap\Gamma^e}\equiv\left(\frac{\partial\phi}{\partial x}\right)\Big|_{\Gamma} \tag{34}$$

Thus, the subdomain integration analog in local element Ω^e reduces to

$$\int_{\Omega_j^e}\left(\frac{\partial^2\phi}{\partial x^2}-\alpha\frac{\partial\phi}{\partial t}\right)d\Omega\stackrel{*}{=}\left(\frac{\partial\phi}{\partial x}\right)\Big|_{\Gamma^e-\Gamma_j^e\cap\Gamma^e}-\int_{\Omega_j^e}\alpha\frac{\partial\phi}{\partial t}d\Omega,\quad j=(e,e+1) \tag{35}$$

where the $\stackrel{*}{=}$ notation in (35) implies an equality due to (34). For $(\alpha,\ \phi)=(\alpha^e,\ \phi^e)$ in Ω^e during a small interval of time Δt,

$$\int_{\Omega_j^e}\left(\frac{\partial^2\phi}{\partial x^2}-\alpha\frac{\partial\phi}{\partial t}\right)d\Omega\stackrel{*}{=}\left(\frac{\partial\phi^e}{\partial x}\right)\Big|_{\Gamma^e-\Gamma_j^e\cap\Gamma^e}-\alpha^e\frac{\partial}{\partial t}\int_{\Omega_j^e}\phi^e\,d\Omega,\quad j=(e,e+1) \tag{36}$$

giving the element matrix system

$$\mathbf{S}^e\boldsymbol{\phi}^e+\mathbf{P}^e[3]\dot{\boldsymbol{\phi}}^e=\left(\frac{\partial\phi^e}{\partial x}\right)\Big|_{\Gamma^e-\Gamma_j^e\cap\Gamma^e}-\alpha^e\frac{\partial}{\partial t}\int_{\Omega_j^e}\phi^e\,d\Omega,\quad j=(e,e+1) \tag{37}$$

where $\mathbf{S}^e$ is as defined in (16), and

$$\mathbf{P}^e[3]=\frac{\alpha^e l^e}{8}\begin{bmatrix}3 & 1\\ 1 & 3\end{bmatrix} \tag{38}$$

Integrated finite difference approach

The integrated finite difference is analogous to the subdomain integration approach for a linear trial function ϕ^e in each element Ω^e except that

$$\int_{\Omega_j^e}\phi^e\,d\Omega\equiv\phi_j\int_{\Omega_j^e}d\Omega \tag{39}$$

Consequently, the element matrix system for solution of the governing PDE in Ω^e is

$$\mathbf{S}^e\boldsymbol{\phi}^e+\mathbf{P}^e[\infty]\dot{\boldsymbol{\phi}}^e=\left(\frac{\partial\phi^e}{\partial x}\right)\Big|_{\Gamma^e-\Gamma_j\cap\Gamma^e}-\alpha^e\frac{\partial\phi^e}{\partial t}\int_{\Omega_j^e}d\Omega,\quad j\in S^e \tag{40}$$

where $\mathbf{S}^e$ is defined by (16), and

$$\mathbf{P}^e[\infty]=\frac{\alpha^e l^e}{2}\begin{bmatrix}1 & 0\\ 0 & 1\end{bmatrix} \tag{41}$$

Nodal domain integration

For the one-dimensional parabolic PDE, the three domain numerical approaches derived above can be represented by a single element matrix system[19]

$$\mathbf{S}^e\boldsymbol{\phi}^e+\mathbf{P}^e[\eta_e]\dot{\boldsymbol{\phi}}^e=\frac{1}{l^e}\begin{bmatrix}1 & -1\\ -1 & 1\end{bmatrix}\begin{Bmatrix}\phi_e\\ \phi_{e+1}\end{Bmatrix}+\frac{\alpha^e l^e}{2[\eta_e+1]}\times\begin{bmatrix}\eta_e & 1\\ 1 & \eta_e\end{bmatrix}\begin{Bmatrix}\dot{\phi}_e\\ \dot{\phi}_{e+1}\end{Bmatrix} \tag{42}$$

where η_e is an element mass lumping factor and determines the Galerkin, subdomain integration, and integrated finite difference domain analogs for $\eta_e=(2,\ 3,\ \infty)$.

For the linear trial function ϕ^e in an irregular triangle and tetrahedron finite elements, the appropriate element matrix systems for two- and three-dimensional linear diffusion problems are readily determined.[20] In the two-dimensional triangle element matrix system, Fig. 2, the two-dimensional element matrix system is

$$\mathbf{S}_2^e\boldsymbol{\phi}^e+\mathbf{P}_2^e[\eta_e]\dot{\boldsymbol{\phi}}^e\equiv\mathbf{0} \tag{43}$$

where the subscript notation indicates a two-dimensional matrix system, and where $\mathbf{S}_2^e$ is a Galerkin approximation for the diffusion component in element Ω^e, and

$$\mathbf{P}_2^e[\eta_e]=\frac{\alpha^e A^e}{3[\eta_e+2]}\begin{bmatrix}\eta_e & 1 & 1\\ 1 & \eta_e & 1\\ 1 & 1 & \eta_e\end{bmatrix} \tag{44}$$

where $A^e=$ area of triangle element, and where $\eta_e=(2,\ 22/7,\ \infty)$ gives the Galerkin, subdomain integration, and integrated finite difference analogs. As in the one-dimensional problem, Dirichlet and Neuman boundary conditions are accommodated analogous to the Galerkin method.

For the three-dimensional tetrahedron element (Fig. 3), the appropriate element capacitance matrix is given by

$$\mathbf{P}_3^e[\eta_e]=\frac{\alpha^e V^e}{4[\eta_e+3]}\begin{bmatrix}\eta_e & 1 & 1 & 1\\ 1 & \eta_e & 1 & 1\\ 1 & 1 & \eta_e & 1\\ 1 & 1 & 1 & \eta_e\end{bmatrix} \tag{45}$$

where $V^e=$ volume of the tetrahedron element, and where $\eta_e=(2,\ 75/23,\ \infty)$ gives the Galerkin, subdomain integration, and integrated finite difference analogs. The element diffusion component is given by the usual Galerkin approximation in element Ω^e.

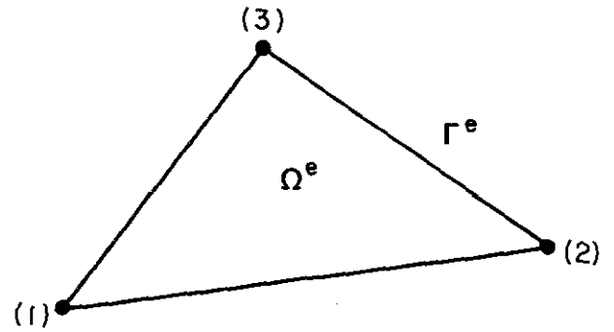

Figure 2(a). Finite element Ω^e with three vertex located nodal points

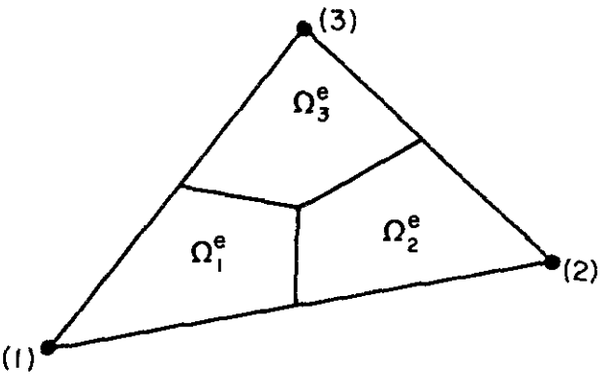

Figure 2(b). Finite element partitioned into nodal domains

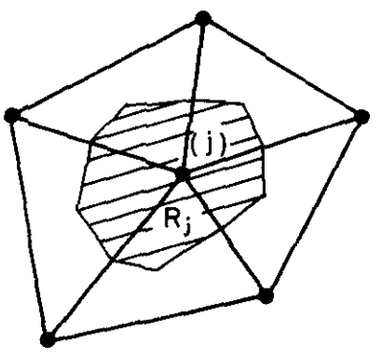

Figure 2(c). Subdomain R_j as the union of all nodal domains associated to nodal point j

IMPROVED MASS MATRIX LUMPING FACTOR

In the previous section, a NDI model is developed for several of the common finite element configurations. The NDI statement is found to represent several numerical approaches by the variation of a mass lumping factor. Numerous mass lumping factors can be determined depending on the approach used to approximate the PDE. Zienkiewicz[16] discusses mass lumping systems and also includes discontinuous trial function approximations in each finite element.

A brief examination of stability and convergence considerations for the family of domain models is given in Appendix A. From Appendix A it is concluded that if a Galerkin analog ($\eta = 2$) and an integrated finite difference analog ($\eta = \infty$) are stable and convergent, then so is the entire range of mass lumped matrix finite element models ($2 \leqslant \eta < \infty$).

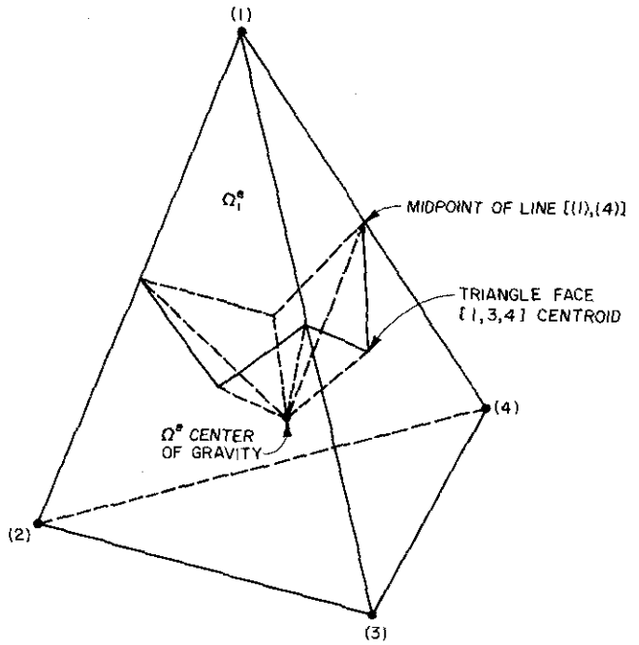

Figure 3. Nodal domain Ω_1^e geometric definition in finite element Ω^e

Approximating complex finite element trial functions with a lower order trial function generates a complete spectrum of possible domain finite element models which can be included into the variable mass lumped formulation. For example, two common approximation norms used in developing such lower order trial function models are the relative error and inner-product norms. Both of these approximation norms can be used to formulate numerous specialized mass lumped finite element models based on some assumed function configuration within each element. Such considerations suggest that an infinity of possible domain numerical models may be produced, each model perhaps providing the 'best' approximation to a particular PDE or a specific class of boundary value problems.

Hromadka and Guymon[6] developed a variable mass-lumped matrix model which allowed a variation of the mass lumping factor with respect to time and between finite elements. However, this variable η scheme involves frequent global matrix regeneration, which results in a relatively high increase in computational effort over a constant η-factor model. Consequently with an infinite number of potential constant-η domain models to choose from, the selection of the constant mass-lumping factor which has the highest probability of producing the best numerical approximation for diffusion problems is needed.

This is the main objective of the paper: to develop such a constant η factor which has the highest probability of reducing the relative approximation error. It can be easily shown that any η-factor model provides a 'best' approximation for some region of a problem domain or for some portion of the simulation. For example, Fig. 4 shows the relative error from various mass-lumped models in the approximation of a classical linear diffusion problem. It can also be shown that these approximations fail to succeed to be the 'best' depending on the problem being considered.

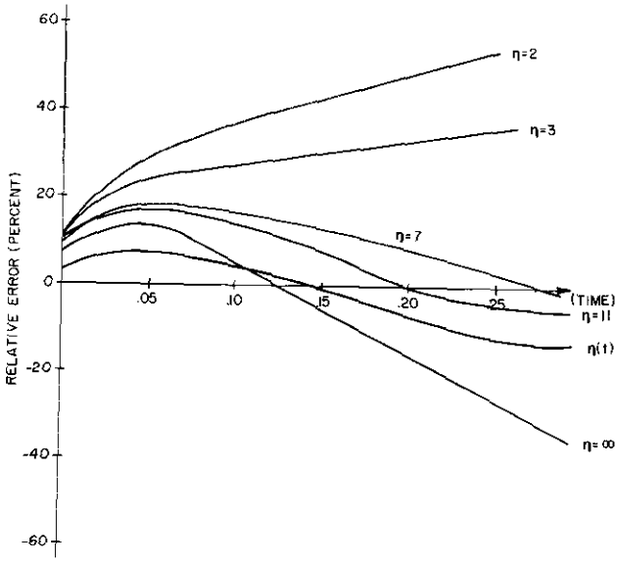

Figure 4. Example integrated relative error in modeling one-dimensional diffusion problem ($\eta=2$: Galerkin; $\eta=3$: subdomain integration; $\eta=\infty$: finite difference, $\eta(t)=$ variable NDI model[6])

In this paper, the approach used to determine an optimum mass weighting factor for the one-dimensional NDI model of equation (42) is based on the Fourier series expansion of an assumed boundary value problem in each control volume of the global domain. For a finite interval R_j (control volume), the usual processes of normalization reduces the governing PDE to the solution of an equivalent PDE on a normalized unit interval

$$\frac{\partial^2\theta}{\partial x^2}=\frac{\partial\theta}{\partial t}, \quad x\in[0,1] \tag{46}$$

where θ is a normalized variable for the PDE state variable, and (x, t) is now defined as normalized space and time. It is assumed in equation (46) that $\theta(x=0)=\theta_{j-1}$, $\theta(x=0.5)=\theta_j$ and $\theta(x=1)=\theta_{j+1}$ where θ_k are the usual nodal values.

The NDI model is based on the well known Crank-Nicolson time advancement procedure to approximate the time derivative of equation (46). The nodal equation for the solution of θ_j is therefore

$$\frac{\Delta t}{2\|R_j\|}[(\theta_{j-1}^{i+1}-2\theta_j^{i+1}+\theta_{j+1}^{i+1})+(\theta_{j-1}^{i}-2\theta_j^{i}+\theta_{j+1}^{i})]$$
$$=\frac{\|R_j\|}{2(\eta_j+1)}[(\theta_{j-1}^{i+1}-\theta_{j-1}^{i})+2\eta_j(\theta_j^{i+1}-\theta_j^{i})$$
$$+(\theta_{j+1}^{i+1}-\theta_{j+1}^{i})] \tag{47}$$

where the normalized length, $\|R_j\|=\frac{1}{2}$; i is the timestep number; and η_j is constant during normalized timestep Δt. Equation (47) evaluates all modeled flux terms at the mid-timestep. For other time derivative approximations, such as forward or backward step differencing, a similar PDE finite difference statement can be developed. An exact solution of the governing PDE at this mid-timestep is

$$\hat{\theta}(x,\epsilon)=-\tfrac{1}{2}(\bar{\theta}_{j-1}-2\bar{\theta}_j+\bar{\theta}_{j+1})\sin\pi x\, e^{-\pi^2\epsilon}$$
$$+(\bar{\theta}_{j+1}+\bar{\theta}_{j-1})x+\bar{\theta}_{j-1} \tag{48}$$

where ϵ is normalized time measured from the mid-timestep; and where $\bar{\theta}=\frac{1}{2}(\theta_j^i+\theta_j^{i+1})$. Equation (48) is a solution to the governing PDE. If it is assumed that all effects of a moving boundary value at $x=(0, 1)$ are equivalent to holding θ constant at the mid-timestep boundary values, then (48) represents an exact solution to the assumed boundary value problem.

The exact Fourier series expansion solution to the proposed boundary value problem, (48), is a good approximation for diffusion problems where the initial condition is a sinusoidal curve. Additionally, (48) is the principal eigenfunction of the boundary value problem since the remaining series terms quickly reduce to zero.[21]

Holding the boundary values of $\hat{\theta}$ constant at the mid-timestep allows a simplification of the NDI nodal equation to

$$\frac{\Delta t}{\|R_j\|}[(\bar{\theta}_{j-1}+\bar{\theta}_{j+1})-(\theta_j^i+\theta_j^{i+1})]\cong\frac{\|R_j\|}{2(\eta_j+1)}$$
$$\times[2\eta_j(\theta_j^{i+1}-\theta_j^i)] \tag{49}$$

Since (48) is assumed exact,

$$\theta_j^i=\hat{\theta}\left(\frac{1}{2},\frac{-\Delta t}{2}\right)=-\tfrac{1}{2}(\bar{\theta}_{j-1}-2\bar{\theta}_j+\bar{\theta}_{j+1})\,e^{\pi^2\Delta t/2}$$
$$+\tfrac{1}{2}(\bar{\theta}_{j-1}+\bar{\theta}_{j+1}) \tag{50}$$

$$\theta_j^{i+1}=\hat{\theta}\left(\frac{1}{2},\frac{\Delta t}{2}\right)=-\tfrac{1}{2}(\bar{\theta}_{j-1}-2\bar{\theta}_j+\bar{\theta}_{j+1})\,e^{-\pi^2\Delta t/2}$$
$$+\tfrac{1}{2}(\bar{\theta}_{j-1}+\bar{\theta}_{j+1})$$

Substituting (50) into (49) and simplifying gives the NDI mass lumping factor

$$\eta_j(\Delta t)=\left\{\frac{4\Delta t(1+e^{-\pi^2\Delta t})}{1-e^{-\pi^2\Delta t}-4\Delta t(1+e^{-\pi^2\Delta t})}\right\} \tag{51}$$

where the normalized timestep Δt is related to the global model timestep $\overline{\Delta t}$ by

$$\Delta t=\frac{\overline{\Delta t}\alpha}{4\|R_j\|^2} \tag{52}$$

Normally Δt is assumed constant for the entire numerical simulation and a single η_j is determined for each finite element. Should Δt vary, then new η_j values may be required according to (51).

From (51), the mass lumping factor varies by

$$8/(\pi^2-8)\leqslant\eta_j(\Delta t)<\infty \tag{53}$$

Equation (51) can be derived by a similar argument applied to other normalized boundary value problems. Inclusion of a time variable (linear polynomial variation) boundary condition adds additional terms to the numerator and denominator of (51), but adds little to change η for small Δt values. Although (51) is a function of the model timestep size, a mass lumped model using the $\eta_j(\Delta t)$ function would be constant with respect to η_j unless the timestep size is changed during the problem simulation.

Comparison of the proposed $\eta_j(\Delta t)$ mass lumped model to other values of mass lumping (e.g. Galerkin, subdomain integration, finite difference) models in the solution of classical boundary value linear diffusion problems will not be presented due to the unavoidable biased selection procedure. That is, it is perhaps more meaningful to express the success of a numerical method in terms of a probability

as determined from numerous simulations, rather than demonstrating the success of the method for a single problem.

A general overview of using the $\eta_j(\Delta t)$ model can be summarized based on the comparison of over 300 computer simulations of several one-dimensional linear diffusion problems using various timestep and element size combinations, as well as different types of boundary conditions.[22] In diffusion problems where the state variable varies rapidly or where a sharp profile exists, a standard lumped mass finite difference analog produces the best results. For slower variations in the state variable and for smoother profiles, the proposed $\eta_j(\Delta t)$ model generally gave the best results. For the fast nodal variation problems, the basic assumptions in deriving the $\eta_j(\Delta t)$ model fail in that the exact solution includes several eigenfunctions beyond the principal eigenfunction used in the $\eta_j(\Delta t)$ model. For the slower nodal variation problems, the Fourier series of eigenfunctions essentially reduces to the principal eigenfunction which is modeled by the assumed boundary value problem in each control volume.

Figure 5 shows a plot of the experimentally determined probability of the $\eta_j(\Delta t)$ model producing the minimum integrated relative error in the solution of several linear diffusion problems. The accuracy of the $\eta_j(\Delta t)$ model was found to decrease as the normalized time-step increases; this observation may be explained by the inaccurate boundary conditions assumed for each control volume problem. It should be noted that although the $\eta_j(\Delta t)$ model was not consistently the best model, in the problems examined where $\eta_j(\Delta t)$ was not the optimum mass lumping factor the resulting model error was generally less than from either the Galerkin finite element or the integrated finite difference models.

The consequences of the above results is that use of the proposed $\eta_j(\Delta t)$ factor should result in a linear diffusion mass matrix lumped finite element model which has a significantly higher occurrence of being the best numerical model. This is important due to the uncertainty of accuracy in any numerical model in the approximation of a PDE where the exact solution is unknown. Once a computer code is prepared based on the NDI variable lumped mass matrix system, it is relatively easy to simulate the particular PDE by each of the more popular domain methods and also by the $\eta_j(\Delta t)$ approach. Such a comparison should aid the analyst in determining a more appropriate discretization of the domain or an adjustment of the timestep in order to reduce the discrepancy between the various mass lumped models and ultimately increase the level of confidence in the final approximation results.

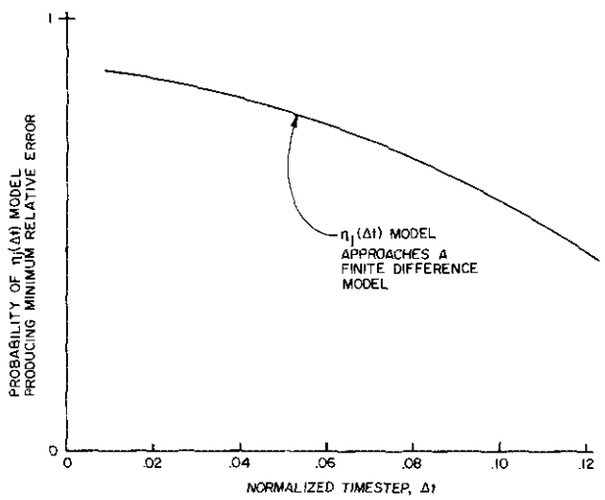

Figure 5. Estimated probability of the $\eta_j(\Delta t)$ model producing minimum integrated relative error for linear diffusion problems (sample of 300 computer simulations)

CONCLUSIONS

The major conclusions from this reasearch are the following:

(1) A unifying numerical model can be developed for many finite element configurations including the one-dimensional, triangle, and tetrahedron finite elements. The unifying model is based on the straight forward nodal domain integration method. The resulting model is found to have the capability of representing the Galerkin finite element, subdomain integration, and integrated finite difference methods by the specification of a single mass matrix lumping factor, η.

(2) The global matrix system composed of the sum of all NDI elements accommodated Dirichlet, Neumann and mixed boundary conditions.

(3) An infinity of possible domain numerical methods are possible. Two methods of developing various mass lumping models are based on the well known relative error and inner-product norms as applied to polynomial trial functions. These models can all be represented by the NDI model for specific values of η.

(4) A computer code based on the Galerkin finite element method can easily be modified to allow a variable mass lumped matrix system and, consequently, represent an integrated finite difference, subdomain integration, and an infinity of other domain methods.

(5) An improved mass lumping factor exists which apparently minimizes approximation error more often than any other domain method. The probability of the proposed optimum mass lumping system being the best numerical method is approximately 85% for small normalized time-step sizes. The improved method is developed based on a linear trial function model and a Crank-Nicolson time advancement approximation. Extension to higher order polynomial trial functions and other time advancement approximations should follow similarly. Although only the one-dimensional problem is considered extension of the approach to multidimensional problems is straightforward.

REFERENCES

1 Bear, J. *Hydraulics of Groundwater Flow*, McGraw-Hill, 1979.
2 Narasimhan, T. N. and Witherspoon, P. A. An integrated finite difference method for analyzing fluid flow in porous media, *Water Resour. Res.* 1976, **12**, 57.
3 Narasimhan, T. N. A perspective on numerical analysis of the diffusion equation, *Adv. Water Resources* 1978, **1**, 3.
4 Narasimhan, T. N., Neuman, S. P. and Witherspoon, P. A. Finite element method for subsurface hydrolgy using a mixed explicit-implicit scheme, *Water Res. Res.* 1978, **14**, 5.
5 Patankar, S. V. *Numerical Heat Transfer and Fluid Flow*, McGraw-Hill, 1980
6 Hromadka II, T. V. and Guymon, G. L. Improved linear shape function model of soil moisture transport, *Water Resour. Res.* 1981a, 17 (3), 504.
7 Kikuchi, Fumio, Notes on the lumped mass approximation for vibration problems, *Proceedings of the 24th Japan National Congress for Applied Mechanics*, University of Tokyo, Japan, 1974.
8 Fried, I. and Malkus, D. S. Finite element mass matrix lumping by numerical integration with no convergence rate loss, *Int. J. Solids Structures* 1974, **11**, 461.

9 Schreyer, H. L. Consistent diagonal mass matrices and finite element equations for one-dimensional problems, *Int. J. Num. Meth. in Eng.* 1978, **12**, 1171.

10 Schreyer, H. L. and Fedock, J. J. Orthogonal base functions and consistent diagonal mass matrices for two-dimensional elements, *Int. J. Num. Meth. in Eng.* 1979, **14**, 1379.

11 Surana, K. S. Consistent mass matrices for three-dimensional beam element due to distributed and lumped non-structural mass systems acting on its span, *Computers and Structures* 1981, **13**, 515.

12 Spalding, D. B. A novel finite-difference formulation for differential expressions involving both first and second derivations, *Int. J. Num. Meth. in Eng.* 1972, **4**, 551.

13 Baliga, B. R. and Patankar, W. V. A new finite-element formulation for convection-diffusion problems, *Numerical Heat Transfer* 1980, **3**, 393.

14 Ramadhyani, S. and Patankar, S. V. Solution of the Poisson equation: comparison of the Galerkin and control-volume methods, *Ist J. for Num. Meth. in Eng.* 1980, **15**, 1395.

15 Hayhoe, H. N. Study of the relative efficiency of finite difference and Galerkin techniques for modeling soil-water transfer, *Wat. Res. Res.* 1978, 14 (1), 97

16 Zienkiewicz, O. C. *The Finite Element Method in Engineering Science*, McGraw-Hill, 1977.

17 Hromadka II, T. V. and Guymon, G. L. A note on numerical approximation of advection-diffusion processes in rectangular domains, *Adv. Water Resources* 1982, **5**, 55.

18 Pinder, G. F. and Gray, W. G. *Finite Element Simulation in Surface and Subsurface Hydrology*, Academic Press, 1977.

19 Hromadka II, T. V. and Guymon, G. L. Some effects of linearizing the unsaturated soil-moisture transfer diffusion model, *Water Resour. Res.* 1980c, **16**, 643.

20 Hromadka II, T. V., Guymon, G. L. and Pardoen, G. Nodal domain integration model of unsaturated two-dimensional soil-water flow: development, *Water Resour. Res.* 1981b, 17 (5), 1425.

21 Myers, G. C. *Analytical Methods in Conduction Heat Transfer*, McGraw-Hill, 1981.

22 McWhorter, D. B and Sunada, D. K. *Groundwater Hydrology and Hydraulics*, Water Resources Publications, 1977.

APPENDIX A: STABILITY AND CONVERGENCE CONSIDERATIONS

Definition: The governing partial differential equation is defined by the description variable Φ as

$$\Phi \equiv \frac{\partial^2 \theta}{\partial x^2} - \frac{\partial \theta}{\partial t}; \quad x \in \Omega \tag{A1}$$

where $\Phi = 0$ is the problem being studied, and initial and boundary conditions are assumed specified according to (46) and (47).

Definition: The $\{\mathbf{S}, \mathbf{P}(\eta)\}$ matrices are defined as follows:

$$\mathbf{S} \equiv \frac{1}{l^e}\begin{bmatrix} 1 & -1 \\ -1 & 1 \end{bmatrix} \tag{A2}$$

$$\mathbf{P}(\eta) \equiv \frac{l^e}{2(\eta+1)}\begin{bmatrix} \eta & 1 \\ 1 & \eta \end{bmatrix} \tag{A3}$$

Definition: The matrix system operation $A(\eta, \phi)$ is defined by

$$A(\eta, \phi) \equiv \mathbf{P}(\eta)\frac{(\phi^{i+1} - \phi^i)}{\Delta t} + \mathbf{S}\frac{(\phi^{i+1} + \phi^i)}{2} \tag{A4}$$

where ϕ^k are vectors of nodal values at time k. $A(\eta, \phi)$ describes a Galerkin, subdomain and finite difference approximation for $\eta = (2, 3, \infty)$ respectively, for the approximation of Φ in Ω.

Theorem: If $A(2)$ and $A(\infty)$ are convergent algorithms to Φ, then $A(\eta)$ is convergent to Φ for $\eta \geq 2$.

Proof: From the definition of $\mathbf{P}(\eta)$

$$\mathbf{P}(\eta) = \left(\frac{3}{\eta+1}\right)\mathbf{P}(2) + \left(\frac{\eta-2}{\eta+1}\right)\mathbf{P}(\infty) \tag{A5}$$

Or

$$\mathbf{P}(\eta) \equiv a_1\mathbf{P}(2) + a_2\mathbf{P}(\infty); \quad a_1 + a_2 = 1 \tag{A6}$$

Therefore

$$A(\eta) = a_1 A(2) + a_2 A(\infty) \tag{A7}$$

and

$$\lim_{\substack{\Delta x \to 0 \\ \Delta t \to 0}} A(\eta) = a_1 \lim_{\substack{\Delta x \to 0 \\ \Delta t \to 0}} A(2) + a_2 \lim_{\substack{\Delta x \to 0 \\ \Delta t \to 0}} A(\infty) \tag{A8}$$

where $A(2)$ and $A(\infty)$ are Galerkin and finite difference approximations. Thus

$$\lim_{\substack{\Delta x \to 0 \\ \Delta t \to 0}} A(\eta) = a_1\Phi + a_2\Phi = \Phi \tag{A9}$$

Theorem: Consider the approximation $A(\eta) = 0$ where η is constant in Ω. Then $A(\eta)$ is stable.

Proof: Rewrite $A(\eta) = 0$ as

$$\left(a_1\mathbf{P}(2) + a_2\mathbf{P}(\infty) + \frac{\Delta t}{2}\mathbf{S}\right)\phi^{i+1} = \left(a_1\mathbf{P}(2) + a_2\mathbf{P}(\infty) - \frac{\Delta t}{2}\mathbf{S}\right)\phi^i \tag{A10}$$

or in global matrix notation

$$G\phi^{i+1} = H\phi^i \tag{A11}$$

For l^e constant in Ω, $a_1P(2)$ determines a tridiagonal matrix

$$a_1P(2) = \frac{a_1 l^e}{6}\begin{bmatrix} 2 & 1 & & & & \\ 1 & 4 & 1 & & & \\ 0 & 1 & 4 & 1 & & \\ \cdots & \cdots & \cdots & \cdots & \cdots & \cdots \\ & & & 1 & 4 & 1 \\ & & & 0 & 1 & 2 \end{bmatrix} \tag{A12}$$

and

$$\frac{\Delta t}{2}S = \frac{\Delta t}{2l^e}\begin{bmatrix} 1 & -1 & & & \\ -1 & 2 & -1 & & \\ 0 & -1 & 2 & -1 & \\ \cdots & \cdots & \cdots & \cdots & \cdots \\ & & -1 & 2 & -1 \\ & & & -1 & 1 \end{bmatrix} \tag{A13}$$

Likewise,

$$a_2P(\infty) = \frac{a_2 l^e}{2}\begin{bmatrix} 1 & 0 & & & \\ 0 & 2 & 0 & & \\ 0 & 0 & 2 & 0 & \\ \cdots & \cdots & \cdots & \cdots & \cdots \\ & & 0 & 2 & 0 \\ & & & 0 & 1 \end{bmatrix} \tag{A14}$$

For $\gamma = \dfrac{\Delta t}{(l^e)^2}$,

$$G = \begin{bmatrix} \left(\frac{a_1}{3}+\frac{a_2}{2}+\frac{\gamma}{2}\right) & \left(\frac{a_1}{6}+\frac{-\gamma}{2}\right) & \\ \left(\frac{a_1}{6}-\frac{\gamma}{2}\right) & \left(\frac{2a_1}{3}+a_1+\gamma\right) & \left(\frac{a_1}{6}-\frac{\gamma}{2}\right) \\ \cdots\cdots & \cdots\cdots & \cdots\cdots \end{bmatrix} \tag{A15}$$

and

$$H = \begin{bmatrix} \left(\frac{a_1}{3}+\frac{a_2}{2}-\frac{\gamma}{2}\right) & \left(\frac{a_1}{6}+\frac{\gamma}{2}\right) & \\ \left(\frac{a_1}{6}+\frac{\gamma}{2}\right) & \left(\frac{2}{3}a_1+a_2-\gamma\right) & \left(\frac{a_1}{6}+\frac{\gamma}{2}\right)\cdots \\ \cdots\cdots & \cdots\cdots & \cdots\cdots \end{bmatrix} \tag{A16}$$

For the specified boundary conditions of Φ: $\theta(x=0, L; t>0)=0$, the (G, H) matrix system becomes a regular tridiagonal matrix system. To show stability, the largest eigenvalue of

$$G^{-1}H \tag{A17}$$

must be less than 1.

For the G matrix,

$$\lambda_G = \left(\tfrac{2}{3}a_1+a_2+\gamma\right) + 2\left(\frac{a_1}{6}-\frac{\gamma}{2}\right)\cos\frac{S\pi}{N-1} \tag{A18}$$

where $N+1$ nodal points are designated between $x=0$ and $x=L$. Then

$$\lambda_G = 1 - 2\left(\frac{a_1}{3}-\gamma\right)\sin^2\left(\frac{S\pi}{2(N-1)}\right) \tag{A19}$$

For the H matrix

$$\lambda_H = \tfrac{2}{3}a_1 + a_2 - \gamma + \left(\frac{a_1}{3}+\gamma\right)\cos\left(\frac{S\pi}{N-1}\right) \tag{A20}$$

or

$$\lambda_H = 1 - \left(\frac{a_1}{3}+\gamma\right)\left(2\sin^2\left(\frac{S\pi}{2(N-1)}\right)\right) \tag{A21}$$

Thus

$$\lambda_{G^{-1}H} = \frac{1 - 2(a_1/3+\gamma)\sin^2(\alpha)}{1 + 2(a_1/3+\gamma)\sin^2(\alpha)}, \qquad S = 1, 2, \ldots, N-1 \tag{A22}$$

where $\alpha = (S\pi)/2(N-1)$. From the above

$$|\lambda_{G^{-1}H}| \text{ is } \leqslant 1 \text{ for all } \gamma \text{ if } a_1 \geqslant 0$$

Theorum: $A(\eta)$ is stable for any distribution of $\eta \geqslant 1$ in Ω.

Proof: This proof will be developed for a nodal point (subdomain) approximation of Φ. For any row p of $A(\eta)$, the following linear equation is determined for solution of nodal value ϕ_p:

$$\left[\left(\mathbf{P}(\eta)+\frac{\Delta t}{2}\mathbf{S}\right)\phi^{q+1} = \left(\mathbf{P}(\eta)-\frac{\Delta t}{2}\mathbf{S}\right)\phi^{q}\right]_p \tag{A23}$$

where p designates nodal values contributing to row p of $A(\eta)$. For row p

$$\mathbf{P}(\eta)\,\phi \equiv \frac{l}{2(\eta+1)}\left[\phi_{p-1} + 2\eta\phi_p + \phi_{p+1}\right] \tag{A24}$$

and

$$\mathbf{S}\phi \equiv \frac{1}{l}\left[-\phi_{p-1} + 2\phi_p + -\phi_{p+1}\right] \tag{A25}$$

Thus, the above gives

$$\begin{aligned} &\frac{1}{2(\eta+1)}\left[\phi_{p-1,q+1} + 2\eta\phi_{p,q+1} + \phi_{p+1,q+1}\right] \\ &\quad + \frac{\Delta t}{2l^2}\left[-\phi_{p-1,q+1} + 2\phi_{p,q+1} - \phi_{p+1,q+1}\right] \\ &\quad = \frac{1}{2(\eta+1)}\left[\phi_{p-1,q} + 2\eta_{p,q} + \phi_{p+1,q}\right] \\ &\quad - \frac{\Delta t}{2l^2}\left[-\phi_{p-1,q} + 2\phi_{p,q} - \phi_{p+1,q}\right] \end{aligned} \tag{A26}$$

Let $\mu = (\eta+1)\,\Delta t/l^2$ and define an error at node p and time q by a Fourier distribution term

$$E_{p,q} \equiv e^{i\beta p h \xi q} \tag{A27}$$

Substituting $E_{p,q}$ into the above gives

$$\begin{aligned} &\left[e^{i\beta(p-1)h\xi q+1} + 2\eta\, e^{i\beta p h\xi q+1} + e^{i\beta(p+1)h\xi q+1}\right] \\ &\quad + \mu\left[-e^{i\beta(p-1)h\xi q+1} + 2\, e^{i\beta p h\xi q+1} - e^{i\beta(p+1)h\xi q+1}\right] \\ &\quad = \left[e^{i\beta(p-1)h\xi q} + 2\eta\, e^{i\beta p h\xi q} + e^{i\beta(p+1)h\xi q+1}\right] \\ &\quad + \mu\left[e^{i\beta(p-1)h\xi q} - 2\, e^{i\beta p h\xi q} + e^{i\beta(p+1)h\xi q}\right] \end{aligned}$$

Dividing through by $e^{i\beta p h\xi q}$ gives

$$\begin{aligned} &\xi\left[e^{-i\beta h} + 2\eta + e^{i\beta h}\right] - \mu\xi\left[e^{-i\beta h} - 2 + e^{i\beta h}\right] \\ &\quad = \left[e^{-i\beta h} + 2\eta + e^{i\beta h}\right] + \mu\left[e^{-i\beta h} - 2 + e^{i\beta h}\right] \end{aligned}$$

But $\cos\beta h = (e^{i\beta h} - e^{-i\beta h})/2$, thus

$$\begin{aligned} \xi[2\cos\beta h + 2\eta] - \mu\xi[2\cos\beta h - 2] &= [2\cos\beta h + 2\eta] \\ &\quad + \mu[2\cos\beta h - 2] \end{aligned} \tag{A30}$$

giving

$$\xi = \frac{(\cos\beta h + \eta) - \mu(1 - \cos\beta h)}{(\cos\beta h + \eta) + \mu(1 + \cos\beta h)} \tag{A31}$$

Stability requires $|\xi| \leqslant 1$ where in the above,

$$\mu \equiv \frac{(\eta+1)\,\Delta t}{l^2}$$

and β is a value of

$$\beta_n \equiv \frac{n\pi}{Nh}, \qquad Nh = L$$

Thus,

$$\xi = \frac{(\cos\beta h + \eta) - 2\mu\sin^2(\beta h/2)}{(\cos\beta h + \eta) + 2\mu\sin^2(\beta h/2)} \tag{A32}$$

The condition $|\xi| \leqslant 1$ requires

$$\left|(\cos\beta h + \eta) - 2\mu\sin^2\frac{\beta h}{2}\right| \leqslant \left|(\cos\beta h + \eta) + 2\mu\sin^2\frac{\beta h}{2}\right| \tag{A33}$$

But for $\cos\beta h + \eta \geqslant 0$, η is greater or equal to one which causes the NDI algorithm to be stable.